

Cite this: *Lab Chip*, 2012, **12**, 627

www.rsc.org/loc

PAPER

## A digital microfluidic method for multiplexed cell-based apoptosis assays

Dario Bogojevic,<sup>ab</sup> M. Dean Chamberlain,<sup>ab</sup> Irena Barbulovic-Nad<sup>ab</sup> and Aaron R. Wheeler<sup>\*abc</sup>

Received 16th September 2011, Accepted 25th November 2011

DOI: 10.1039/c2lc20893h

Digital microfluidics (DMF), a fluid-handling technique in which picolitre-microlitre droplets are manipulated electrostatically on an array of electrodes, has recently become popular for applications in chemistry and biology. DMF devices are reconfigurable, have no moving parts, and are compatible with conventional high-throughput screening infrastructure (*e.g.*, multiwell plate readers). For these and other reasons, digital microfluidics has been touted as being a potentially useful new tool for applications in multiplexed screening. Here, we introduce the first digital microfluidic platform used to implement parallel-scale cell-based assays. A fluorogenic apoptosis assay for caspase-3 activity was chosen as a model system because of the popularity of apoptosis as a target for anti-cancer drug discovery research. Dose-response profiles of caspase-3 activity as a function of staurosporine concentration were generated using both the digital microfluidic method and conventional techniques (*i.e.*, pipetting, aspiration, and 96-well plates.) As expected, the digital microfluidic method had a 33-fold reduction in reagent consumption relative to the conventional technique. Although both types of methods used the same detector (a benchtop multiwell plate reader), the data generated by the digital microfluidic method had lower detection limits and greater dynamic range because apoptotic cells were much less likely to de-laminate when exposed to droplet manipulation by DMF relative to pipetting/aspiration in multiwell plates. We propose that the techniques described here represent an important milestone in the development of digital microfluidics as a useful tool for parallel cell-based screening and other applications.

### Introduction

The first steps of drug discovery involve screening compounds in two stages.<sup>1–3</sup> In the first stage, a large library ( $>10^4$  compounds) of potential drugs is screened using cell-free biochemical assays to identify candidates that elicit a desirable response (*e.g.*, inhibition of an enzyme). After identifying hits (and after some optimization), the second stage is implemented, in which a much smaller group of compounds is screened in cell-based assays, which allows for the elimination of candidates from the pipeline that have problematic properties (*e.g.*, toxicity, solubility or permeability concerns, *etc.*). It is widely recognized that the discovery process is more efficient if the cell-based assays are introduced as early as possible to eliminate false leads, leading to the mantra, “fail early, fail cheaply”.<sup>4</sup> But this strategy is not widely used, because cell-based assays are much more expensive and complex than their cell-free assay equivalents. Thus, there is great interest in new technologies that make cell-based assays less

expensive and thus more feasible for high-throughput screening in early stage drug discovery.<sup>5</sup>

One promising approach to reducing the costs and complexity of cell-based assays is microfluidics,<sup>6–14</sup> a technology based on interconnected micron-dimension channels. Although microchannels have been widely used in experiments with cells, most such experiments have required a customized microscope-based readout, and in fact, it is difficult to integrate such methods with plate readers that are commonly used in high throughput screening<sup>15</sup> (with notable exceptions<sup>16</sup>). Another drawback is the lack of reconfigurability – different assays often require different channel layouts, which requires users to incur significant costs in time and resources to fabricate new devices.<sup>17</sup> An alternative approach to the challenge of miniaturizing cell-based assays that solves some of the drawbacks associated with microchannels is the use of digital microfluidics, a reconfigurable fluid handling technique that is easily integrated with microplate readers and other conventional detectors.

Digital microfluidics (DMF) is a technology in which individual picolitre-microlitre-sized droplets are manipulated by applying electric fields to an array of electrodes covered by a hydrophobic dielectric coating. Sample droplets can be dispensed from reservoirs, moved, merged and split with no need for tubes or channels.<sup>18</sup> Because DMF features a two-dimensional array configuration it is a good match for array-based

<sup>a</sup>Institute for Biomaterials and Biomedical Engineering, University of Toronto, 164 College St., Toronto, ON, M5S 3G9, Canada

<sup>b</sup>Donnelly Centre for Cellular and Biomolecular Research, 160 College St., Toronto, ON, M5S 3E1, Canada

<sup>c</sup>Department of Chemistry, University of Toronto, 80 St George St., Toronto, ON, M5S 3H6, Canada. E-mail: aaron.wheeler@utoronto.ca; Fax: +1 (416) 946 3865; Tel: +1 (416) 946 3864

biochemical applications.<sup>19,20</sup> Recent applications of DMF include proteomic sample preparation,<sup>21–24</sup> enzyme assays,<sup>25–27</sup> polymerase chain reaction,<sup>28,29</sup> immunoassays,<sup>30–32</sup> clinical sample processing<sup>33</sup> and applications involving cells.<sup>34–41</sup> The latter category is particularly appealing, as the capacity to analyze small numbers of cells in a two-dimensional array seems a good match for application to pharmaceutical screening assays in which cells are challenged with constituents of a chemical library to find hits with desirable phenotypic effects.

Most of the previous work using digital microfluidics for applications involving cells used non-adherent cells suspended in droplets. We recently reported the first DMF methods compatible with adherent cells<sup>37</sup> (and others have adopted similar techniques<sup>40</sup>); these applications necessitated the development of patterned, heterogeneous devices designed to facilitate cell growth in some regions, and droplet manipulation in others. This is an important development, as most cells used for screening in the pharmaceutical industry are adherent. Here, we build on our initial work to report the first DMF-enabled screening assay on adherent cells. With an eye towards future applications in the pharmaceutical industry, the results reported here were generated using a standard, bench-top fluorescence plate reader.

Apoptosis was chosen as a model system for this work, because it is associated with many types of cancer,<sup>42,43</sup> which has made it a popular target in anti-cancer drug discovery.<sup>44</sup> Moreover, cell-based apoptosis assays are a particularly attractive target for new technologies, because of the tendency of apoptotic cells to delaminate from surfaces, which makes cell-based assays in conventional formats nearly impossible. An early hallmark of apoptosis is the activation of caspase enzymes.<sup>45</sup> Here, we report the development of a multiplexed DMF-enabled screen to evaluate caspase-3 activity in apoptotic cells. We use the term “multiplex” to refer to an assay in which several cell samples are exposed to varying concentrations of drug at the same time (as opposed to previous DMF studies evaluating only one condition at a time<sup>34</sup>). The results obtained using the DMF platform were compared with those obtained using standard multiwell plate techniques. In addition to the advantages in reagent consumption and ease of analysis, the digital microfluidic method proved to be particularly useful for gentle delivery of reagents and other solutions to cells, resulting in very little cell de-lamination from the surfaces. We propose that the techniques described here represent an important milestone in the development of digital microfluidics platform as a useful tool for cell-based screening and other applications.

## Experimental

### Reagents

Unless noted otherwise, general-use reagents were from Sigma Aldrich Canada (Oakville, ON) and cell culture reagents were from Invitrogen/Life Technologies (Burlington, ON). All reagents, washing solutions and media used in experiments with the DMF devices contained 0.05% Pluronic F68 (w/v).<sup>46</sup> Stock solutions of staurosporine were dissolved in DMSO before diluting. Parylene-C dimer was from Specialty Coating Systems (Indianapolis, IN), and Teflon-AF was purchased from DuPont (Wilmington, DE).

### DMF device fabrication and assembly

Digital microfluidic devices were fabricated in the University of Toronto Emerging Communications Technology Institute (ECTI) cleanroom facility, using a transparent photomask printed at Pacific Arts and Design (Markham, ON). Digital microfluidic device bottom plates bearing patterned chromium electrodes were formed by photolithography and etching as described previously,<sup>37</sup> and were coated with 7  $\mu\text{m}$  of Parylene-C and 50 nm of Teflon-AF. Parylene-C was applied using a vapor deposition instrument, and Teflon-AF was spin-coated (1% wt/wt in Fluorinert FC-40, 1600 rpm, 60 s) followed by post-baking on a hot-plate 160  $^{\circ}\text{C}$ , 10 min). The polymer coatings were removed from contact pads by gentle scraping with a scalpel to facilitate electrical contact for droplet actuation. As depicted in Fig. 1a, the electrode design on the bottom plate featured six assay zones spaced 9 mm apart formed from 72 actuation electrodes (polygons with area  $\sim 4.9 \text{ mm}^2$  ea.) and 12 reservoir electrodes (polygons with area  $\sim 33.1 \text{ mm}^2$  ea.), with inter-electrode gaps of 35–130  $\mu\text{m}$ . Fifteen pairs of analogous electrodes were bussed (electrically connected) between the assay zones to decrease number of driving signals required.

DMF device top plates were formed from indium tin oxide (ITO) coated glass substrates (Delta Technologies Ltd, Stillwater, MN). These substrates were globally coated with 50 nm Teflon-AF, which was patterned by lift-off to feature an array of six 1.5 mm diameter circular regions of exposed ITO (known as “hydrophilic sites”) using a method developed for this purpose.<sup>47</sup> As shown in Fig. 1b, devices were assembled with an ITO-glass top plate and a chromium-on-glass bottom plate separated by a spacer formed from 2 pieces of double-sided tape (total spacer thickness 140  $\mu\text{m}$ ), such that a hydrophilic site on the top plate

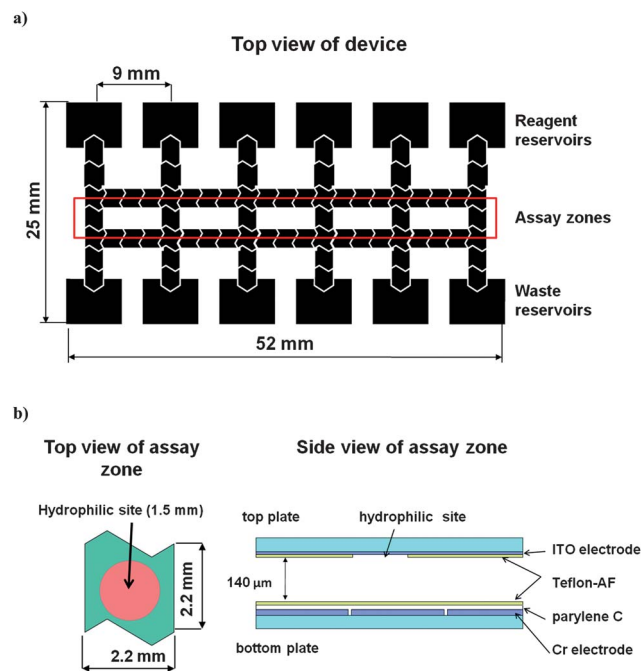


**Fig. 1** DMF device used for multiplexed cell-based assays. a) Top-view schematic of full device bearing six assay zones. b) Top- and side-view schematics of one assay zone.

was aligned over a central electrode on each assay zone. Moreover, each  $\sim 75 \text{ mm} \times 25 \text{ mm}$  top plate was oriented such that the top-plate edges roughly aligned with the outer-edges of the reservoir electrodes on the bottom plate.

### DMF device operation

Driving potentials (200–250  $V_{pp}$ ) were generated by amplifying the output of a function generator (Agilent Technologies, Santa Clara, CA) operating at 15 kHz and were applied between the top electrode (ground) and sequential electrodes on the bottom plate *via* the exposed contact pads. Five common operations were performed on assembled DMF devices in “standard” orientation (*i.e.*, bottom plate on the bottom, top plate on the top). *Reservoir loading*:  $\sim 6 \mu\text{L}$  aliquots were loaded into reservoirs on assembled DMF devices by simultaneously pipetting an aliquot onto the bottom plate at the edge of the top plate, and simultaneously applying driving potential to the closest reservoir electrode (relative to the ITO electrode on the top plate) to draw the fluid into the reservoir. *Active dispensing from reservoirs*:  $\sim 1 \mu\text{L}$  droplets were actively dispensed from reservoirs onto actuation electrodes by actuating sequential electrodes adjacent to the reservoirs<sup>48</sup> (Fig. 2, Frames 1–2). *Passive dispensing*: when  $\sim 1 \mu\text{L}$  droplets were actuated across dry hydrophilic sites,  $\sim 0.3 \mu\text{L}$  sub-droplets were formed at the sites by passive dispensing (Fig. 2, Frames 3–4). *Passive solution exchange*: when  $\sim 1 \mu\text{L}$  droplets were actuated across wet hydrophilic sites,  $\sim 0.3 \mu\text{L}$  sub-droplets were formed, displacing the old solution (Fig. 2, Frames 6–7). *Active dispensing from hydrophilic sites*: in some experiments, large-volume droplets were formed on hydrophilic sites by merging separate  $0.3 \mu\text{L}$  and  $1 \mu\text{L}$  droplets. Under these conditions, the excess volume was actively dispensed away from the hydrophilic sites by actuating the electrodes adjacent to them (moving  $\sim 1 \mu\text{L}$  away from the site and leaving  $\sim 0.3 \mu\text{L}$  on the site).

### Macro-scale cell culture

Complete cell culture medium was formed from high-glucose DMEM supplemented with 10% fetal bovine serum (FBS), 100 units/mL penicillin, and  $100 \mu\text{g mL}^{-1}$  streptomycin. HeLa cells (human cervical adenocarcinoma cell line) were grown to near confluency in complete medium in T-25 flasks in an incubator at  $37^\circ\text{C}$  with 5%  $\text{CO}_2$ . At the beginning of each experiment, cells were detached using a solution of trypsin (0.25% w/v) and EDTA (1 mM), centrifuged, then resuspended in complete medium containing 0.05% Pluronic F68 (w/v) at the appropriate density.

### Cell-spreading assay

A two-plate chamber (similar to a DMF device) was used to assess cell spreading on ITO. Briefly, ITO-glass substrates coated with Teflon-AF bearing 2 mm diameter circular regions of exposed ITO were formed as above to serve as the bottom plate.  $2 \mu\text{L}$  aliquots of complete media containing approximately 500 cells were pipetted onto the exposed ITO regions. A glass microscope slide uniformly coated with 50 nm Teflon-AF was then affixed as a top plate, separated from the bottom plate by a  $300 \mu\text{m}$  thick spacer formed from double-sided tape. The assembled setup was then stored in a Petri dish containing DI

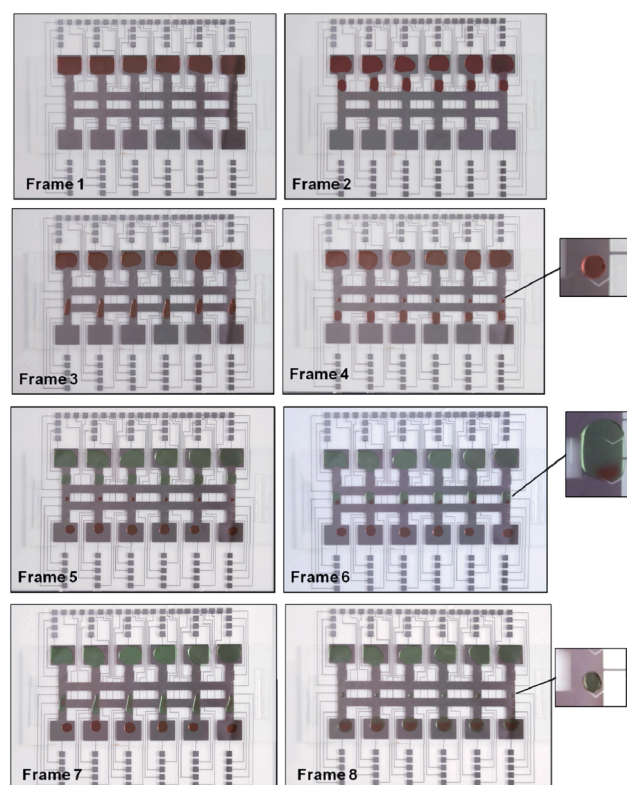


**Fig. 2** Series of frames from a movie depicting the droplet operations used to implement a 6-plex apoptosis assay on a DMF device. Frames 1 and 2 illustrate dispensing droplets containing cells from reservoirs, and Frames 3 and 4 subsequent seeding onto dry (non-occupied) hydrophilic sites by passive dispensing. Frames 5–8 illustrate a similar process for reagent exchange on wet (occupied) hydrophilic sites; this process was used sequentially to deliver candidate drugs, fluorescent dyes, and rinse solutions to the cells. The droplets in this figure contained colored dyes for visualization.

$\text{H}_2\text{O}$  in a cell culture incubator. For comparison,  $100 \mu\text{L}$  aliquots of complete media containing approximately 5,000 cells were pipetted into wells in 96-well plates with flat, transparent polystyrene (PS) bottom surfaces (Greiner Bio-One, Germany) and stored in a cell culture incubator. The ITO chambers and well plates were periodically removed from the incubator to assess cell density and spreading using an Axiovert inverted microscope (Carl Zeiss). At least five replicates were evaluated for each condition. Cell areas were determined using ImageJ software (US National Institutes of Health).

### Caspase-3 assay

A three-step procedure was developed to reproducibly implement cell-based apoptosis assays. *Step 1*: six aliquots of cells in complete media ( $2 \times 10^6$  cells  $\text{mL}^{-1}$ ) were loaded into reservoirs, actively dispensed from reservoirs, and then passively dispensed onto dry hydrophilic sites as described above. Each  $\sim 0.3 \mu\text{L}$  sub-droplet positioned on a hydrophilic site contained  $\sim 800$  cells. Waste and unused reservoir fluids were removed by pipette, and devices were flipped upside down (*i.e.*, top plate on the bottom) and stored in a humidified chamber in an incubator overnight. Devices were removed from the incubator and flipped to

standard orientation. *Step 2*: aliquots of staurosporine (ST, 0, 1.25, 2.5, 5, or 10  $\mu\text{M}$  in high-glucose DMEM supplemented with 1% FBS) were loaded into reservoirs. Two droplets of ST per each assay zone were actively dispensed from reservoirs and passively exchanged onto the cell-bearing hydrophilic sites. A third set of ST droplets was then actively dispensed and merged with the cell-containing droplet forming combined volume droplets of 1.3  $\mu\text{L}$  each. Waste and unused reservoir fluids were removed by pipette, and devices were flipped and stored in a humidified chamber in an incubator for 5 h. Devices were removed from the incubator, flipped to standard orientation, and six  $\sim 1$   $\mu\text{L}$  droplets were actively dispensed away from the hydrophilic sites to waste reservoirs. *Step 3*: a procedure identical to that described for step 2 was implemented, but with 5  $\mu\text{M}$  NucView 488 (Biotium Inc., Hayward, CA) in PBS and an incubation time of 45 min. In some experiments, an extra step (*step 2B*) was included between steps 2 and 3, in which a procedure identical to that described for step 2 was implemented, but with 10  $\mu\text{M}$  Ac-DEVD-CHO (Biotium Inc.) in PBS and an incubation time of 30 min.

For comparison, apoptosis assays were implemented in 96-well plates. Briefly, 100  $\mu\text{L}$  aliquots of cells in complete media at  $2 \times 10^5$  cells  $\text{mL}^{-1}$  ( $\sim 20,000$  cells/well) were dispensed into wells and incubated overnight. The old media was removed by pipette and replaced with 100  $\mu\text{L}$  aliquots of ST (same concentrations as DMF) and incubated for 5h. The old reagents were then removed by pipette and replaced with 100  $\mu\text{L}$  aliquots of 5  $\mu\text{M}$  NucView 488 in PBS and incubated for 45 min.

Fluorescence intensities for assays implemented on DMF devices and in well plates were measured using a multiwell plate reader (Pherastar, BMG Labtech, Cary, NC) with 6 mm diameter circular read sites (each with a  $15 \times 15$  point matrix and 10 flashes per point), automatic gain and focus adjustments, and  $\lambda_{\text{ex}}/\lambda_{\text{em}} = 485/520$  nm. Well plates were simply inserted into the reader, and DMF devices were positioned on top of 96 well plates (aligned with droplets at the center of corresponding wells) prior to insertion. Each experimental condition was replicated at least six times, and One-Way ANOVA with a Tukey's pos-hoc test was implemented using Origin (OriginLab, Northampton, MA). In some cases, cells in DMF devices in various stages of the above experiments were imaged using reflective fluorescence and bright-field microscopy on a DM2000 upright microscope (Leica Microsystems Canada, Richmond Hill, ON).

### Cell wash assay

A four-step assay was developed to investigate the effects of washes on cells that are undergoing apoptosis. *Step 1* was identical to step 1 from the caspase-3 assay (above). *Step 2*: Six aliquots of 10  $\mu\text{M}$  ST in high-glucose DMEM supplemented with 1% FBS were loaded into reservoirs, and two droplets per each assay zone were actively dispensed from reservoirs and passively exchanged onto the cell-bearing hydrophilic sites. Devices were flipped and stored in a humidified chamber in an incubator for 6 h. Devices were removed from the incubator flipped to standard orientation. *Step 3*: Six aliquots of nuclear stain, Hoechst 33342 (5  $\mu\text{g ml}^{-1}$  in PBS) were loaded into reservoirs. One droplet per assay zone was actively dispensed from reservoirs and merged with the cell-containing droplet forming combined volume

droplets of 1.3  $\mu\text{L}$  each. Devices were flipped, stored in a humidified chamber in an incubator for 30 min, retrieved and returned to standard orientation, and imaged using reflective fluorescence microscopy with  $\lambda_{\text{ex}}/\lambda_{\text{em}} = 350/461$  nm. The excess volume ( $\sim 1$   $\mu\text{L}$ ) was actively dispensed away from the hydrophilic sites to waste reservoirs. *Step 4*: Six aliquots of PBS were loaded into reservoirs. Four  $\sim 1$   $\mu\text{L}$  wash droplets per each assay zone (in series) were actively dispensed from reservoirs and passively exchanged onto the cell-bearing hydrophilic sites with imaging between successive wash steps. Cell numbers were determined with ImageJ software using the Analyse particles tool. At least six replicates were evaluated before and after each wash step.

## Results and discussion

### Device and method development

In this paper, we introduce the first DMF platform used to implement multiplexed cell-based assays of the kind commonly used in drug discovery. We used this method to generate dose-response profiles of caspase-3 activity as a function of staurosporine concentration. The device design shown in Fig. 1 was developed to facilitate cell growth in some regions, and droplet manipulation in others. The device consists of reagent reservoirs, six assay zones, waste reservoirs and actuation electrodes with appropriate contact pads. As shown, each assay zone centered around a hydrophilic site on the top plate, which served as the substrate for cell seeding, growth, and analysis. Analogous electrodes were electrically connected between the assay zones to decrease number of driving signals required. All of the data presented here was generated in six-plex experiments, in which six assays were conducted simultaneously. We note that the device design depicted in Fig. 1 is proof-of-concept, and requires that reservoirs be used (at different times) to contain different reagents. We anticipate that future designs will include separate reservoirs dedicated to different reagents.

Four types of droplet dispensing mechanisms were optimized and used to implement apoptosis assays. The first mechanism, active dispensing from reservoirs (Fig. 2, frames 1–2), was performed by actuating the electrodes adjacent to a reservoir in series, which causes the reservoir volume to neck and then pinch into a unit droplet.<sup>48</sup> The second and third mechanisms, passive dispensing<sup>37</sup> (Fig. 2, Frames 3–4) and passive solution exchange (Fig. 2, Frames 6–7), were implemented by electrostatically driving droplets across the hydrophilic sites on the surface of the top-plate, which results in spontaneous formation of sub-droplets known as virtual microwells.<sup>47</sup> Finally, a fourth mechanism, active dispensing from a hydrophilic site, was used to move excessive volume away from the virtual microwells. In between each of these steps, devices were inverted and placed in the incubator for “upside-down” cell culture.<sup>41</sup> Detailed descriptions of each of these operations are recorded in the experimental section.

Cells were seeded and grown on hydrophilic sites patterned on Teflon-AF coated top plates of DMF devices. In previous work, hydrophilic sites for cell adhesion on DMF devices were formed by adsorption of proteins<sup>37</sup> or peptides<sup>40</sup> to the bottom plate

surface. In initial work for the experiments described here, we used similar methods to form hydrophilic sites; however, such sites led to unacceptable levels of variance in the number of cells seeded. In response to this challenge, we developed a new method that enables repeatable and uniform fabrication of hydrophilic sites, using lift-off to form circular regions of exposed ITO for cell seeding and growth (Fig. 3a). As described elsewhere,<sup>47</sup> passive dispensing on hydrophilic sites formed using this technique result in much more uniform densities when applied to cell seeding and culture.

A critical question for the new method was the suitability of ITO as a substrate for cell growth. Previous studies have reported the successful culture of various cell lines on ITO surfaces.<sup>41,47,49–52</sup> Cell attachment is one of the factors that can influence cells to undergo apoptosis; therefore, HeLa cell attachment and spreading characteristics on ITO were evaluated and compared to widely used treated polystyrene (PS) surfaces. In qualitative tests, the morphologies of cells grown on the two substrates were similar (Fig. 3a and inset). More importantly, quantitative measurements of cell spreading (Fig. 3b) confirm that there is no significant difference between the two substrates. Thus, ITO is an appropriate substrate for the model system reported here, and is likely a suitable substrate for other cell-based assays in which cell attachment and spreading are important parameters.

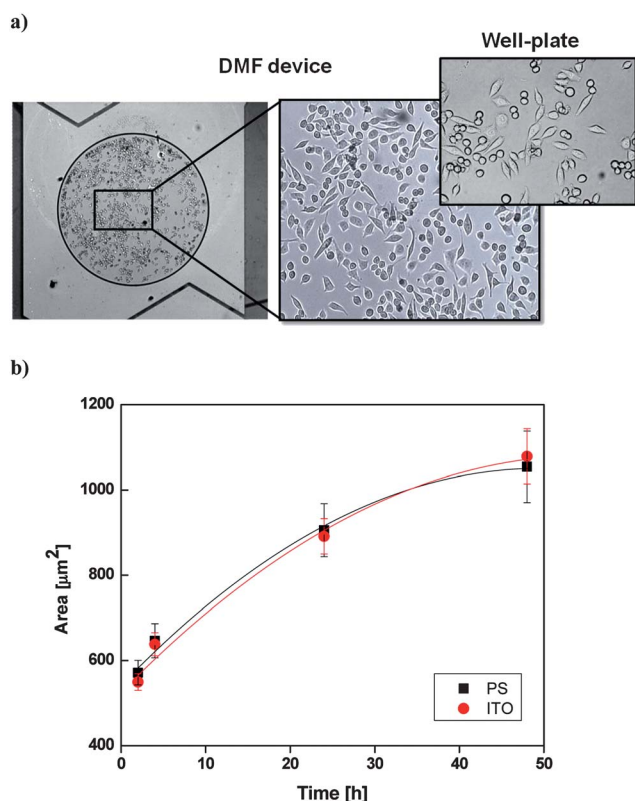


**Fig. 3** Cell spreading on DMF devices. a) Pictures of HeLa cells on a hydrophilic site on a DMF device and (inset) a picture of cells grown on a PS well-plate. b) Cell areas as a function of time on PS and ITO surfaces. Each point represents mean value of cell area for at least 20 cells in 5 different pictures. The error bars represent one standard deviation.

### Apoptotic cell loss

A particular challenge with apoptosis assays is prevention of cell de-lamination from the culture surface. A morphological characteristic of apoptosis is loss of cell attachment and apoptotic cells can be easily detached from culture surfaces during wash steps. This, in turn, can lead to loss of information, data inconsistency and irreproducibility. Thus, cell loss can be a major bottleneck in developing an apoptotic assay that requires wash steps. Wash steps are the exchange of used reagents with fresh solution, such as PBS, and they are often executed multiple times (in series) to ensure complete solution exchange. Here, we examined apoptotic cell loss as a function of washing in two systems: standard 96-well plates and DMF devices.

In multiwell plates, wash steps are implemented by aspiration and dispensing of solutions using a pipette. In tests of cells undergoing apoptosis in multiwell plates, after the first wash, 13% of cells were lost (not shown), and second wash resulted in a loss of 38% cells (Fig. 4). The wash steps in the 96-well plate resulted in large variation in cell number from well to well which is reflected in the large standard deviations. On DMF devices, wash steps were performed using passive solution exchange as in Fig. 2, frames 6–7. As shown in Fig. 4, no significant cell loss was

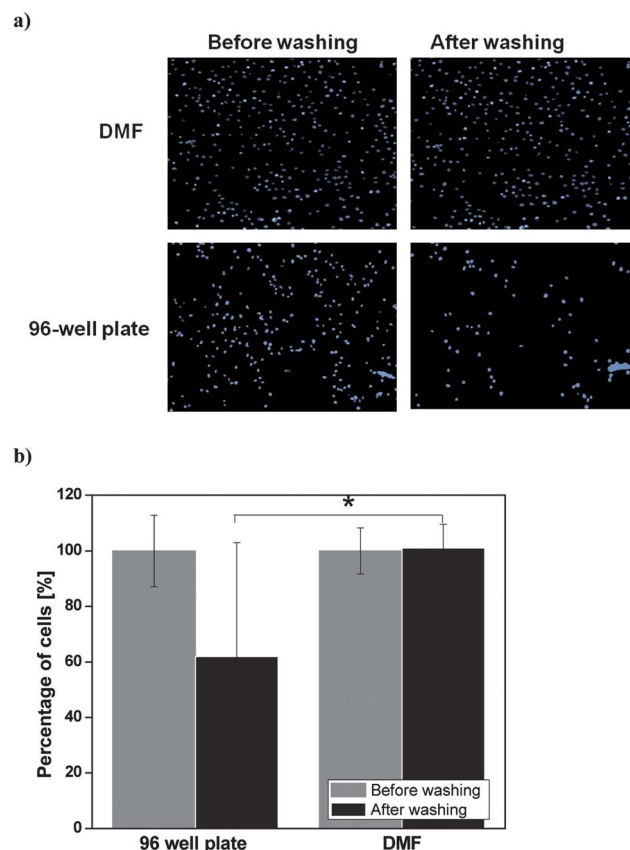


**Fig. 4** Apoptotic cell losses after washing. a) Pictures of apoptotic cells before and after two successive washing steps in a 96 well plate and on a DMF device. b) Graph depicting the number of cells in a 96-well plate and a DMF device before and after washing. The asterisk, \*, denotes that the mean difference between DMF and 96 well plate after washing steps is significant ( $p < 0.05$ ). The error bars represent one standard deviation.

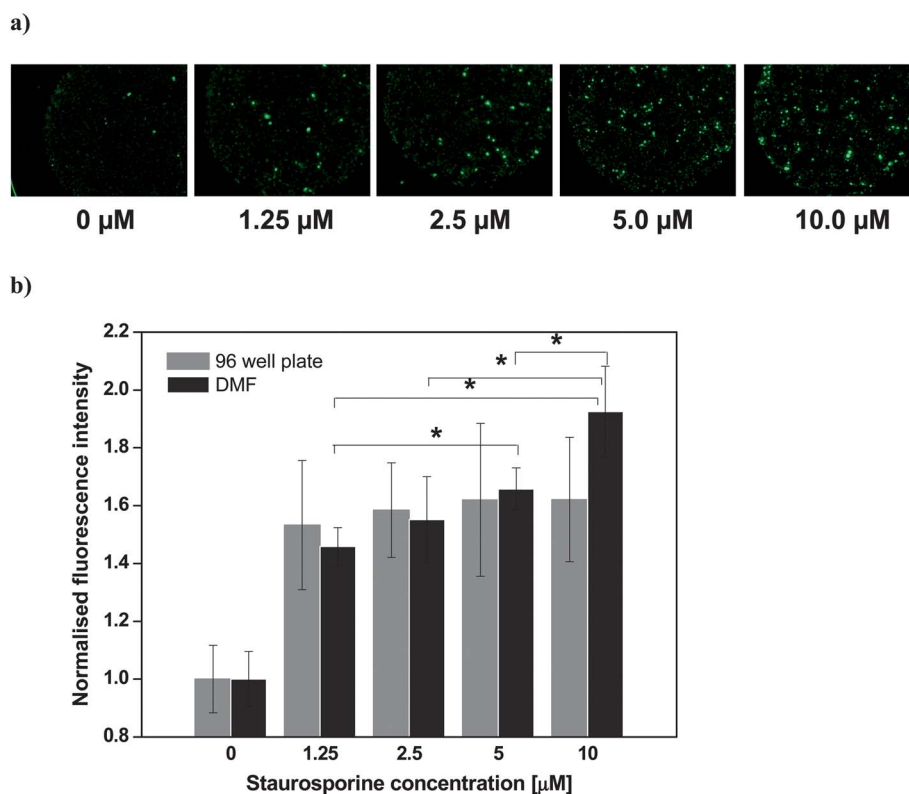


**Fig. 5** Caspase-3 activity in HeLa cells treated with different concentrations of staurosporine. a) Images of cells stained with NucView 488 caspase-3 substrate for different concentrations of staurosporine on a DMF device. b) Fluorescence intensity as a function of staurosporine concentration originating from cells assayed on a 96 well plate and on the DMF device normalised to the intensities of cells not exposed to staurosporine. An asterisk, \*, denotes cases for which the difference is significant ( $p < 0.05$ ). The mean differences between untreated cells (0  $\mu\text{M}$  ST) and cells exposed to all other ST concentrations are significant for both DMF and 96-well plate assays (these relationships are not marks on the graph for clarity). The error bars represent one standard deviation.

found on the DMF device after two consecutive wash steps. This indicates that there is low or negligible shear stress exerted on the cells attached to the exposed ITO. We propose that this is a result of the extensive flow recirculation in droplets manipulated by DMF,<sup>53</sup> which is likely associated with low shear stress near the droplet/surface interface. Regardless, the gentle wash steps implemented by DMF retain the weakly adhered apoptotic cells. We propose that this feature of DMF platforms is a useful advantage over the standard well plate methods for cell-based assays.

### Caspase-3 assay

Caspase-3 is a primary member of the executioner caspase family. During apoptosis, up-regulation of caspase-3 triggers the enzymatic degradation of numerous proteins inside the cell, resulting in morphological changes characteristic of apoptosis.<sup>54</sup> The activation of caspase-3 usually results in the irreversible commitment of a cell to apoptosis, and the inhibition of caspase-3 by synthetic peptide inhibitors often prevents apoptosis induced by various stimuli.<sup>55</sup> Thus, the detection of caspase-3 activation is frequently used as a marker for cells undergoing apoptosis. In the work reported here, a cell membrane-permeable fluorogenic enzyme substrate, NucView, was used for caspase-3 detection. This substrate does not require cell lysis and facilitates

detection of caspase-3 activity within intact cells; therefore, it is suitable for live cell-based assays.<sup>56</sup> Staurosporine is a well-known agonist for caspase-3 activity, and thus was chosen as the model drug for this study.

A NucView assay was adapted for use with digital microfluidics. Cells were seeded and grown, exposed to staurosporine, and then stained with NucView. The six-plex device format was useful for simultaneous evaluation of six different concentrations of staurosporine; representative fluorescence images of cells on different sites on a device are shown in Fig. 5a. As expected, the signal increased as a function of staurosporine concentration. As far as we are aware, this is the first example of the implementation of a cell-based assay of the type used in drug discovery by digital microfluidics. As a benchmark for the digital microfluidic method, comparable assays were carried using conventional techniques (*i.e.*, pipetting, aspiration, and 96-well plates). Because of the reduction in volumes, the DMF method was associated with a 33-fold decrease in reagent consumption (*i.e.*, media, staurosporine, and NucView).

Fluorescence intensity for the apoptosis assay was measured using a benchtop multiwell plate reader with identical settings for both the DMF device and 96-well plate assays, and dose-response curves are shown in Fig. 5b. As expected, because of cell de-lamination during the process of delivering reagents and washing (see above), the data generated using conventional

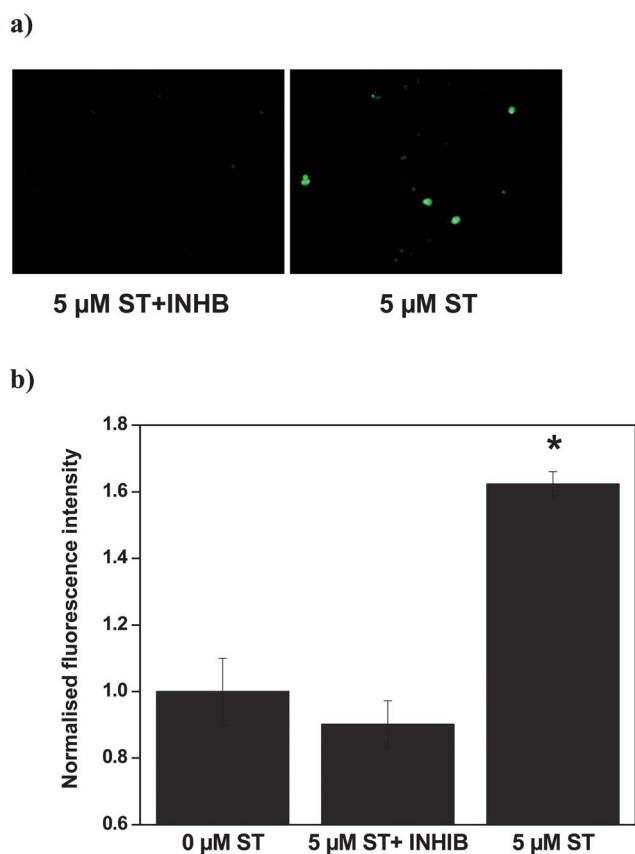


**Fig. 6** Test of specificity of NucView 488 substrate for caspase-3 on a DMF device. Cells were made apoptotic by exposure to 5  $\mu\text{M}$  ST, and prior to adding NucView, some cells were incubated with Caspase-3 inhibitor Ac-DEVD-CHO for 30 min. a) Images of cells treated with caspase-3 inhibitor (5  $\mu\text{M}$  ST + INHB) and cells treated with 5  $\mu\text{M}$  ST alone. b) Fluorescence intensities normalised to those of untreated cells (0  $\mu\text{M}$  ST). An asterisk, \*, denotes that the mean difference is significant compared to other two values ( $p < 0.05$ ). Error bars represent one standard deviation.

techniques were poor. Specifically, the measured fluorescence intensities were nearly identical (and were associated with large standard errors) for cells exposed to all non-zero concentrations of ST. In contrast, assays implemented on the DMF platform had reduced standard errors, and the different concentrations of staurosporine were associated (in most cases) with significantly different fluorescence intensities. Specifically, the signals originating from 10 and 5  $\mu\text{M}$ , 10 and 2.5  $\mu\text{M}$ , 10 and 1.25  $\mu\text{M}$ , and 5 and 1.25  $\mu\text{M}$  staurosporine were all significantly different ( $p < 0.05$ ). Thus, the quality of the data generated using the DMF method was far superior, which suggests particular utility for DMF in cell-based screening assays in which cells are weakly adhered to the surface.

The specificity of the NucView substrate was validated using the cell-permeable caspase-3 inhibitor Ac-DEVD-CHO. As described in the methods section, a 60-droplet-dispensing method (1 droplet of cells, 3 droplets of ST, 3 droplets of inhibitor, and 3 droplets of NucView for each of six analysis sites) was developed and applied to cells grown on hydrophilic sites. As shown in Fig. 6, the inhibitor prevented the NucView substrate cleavage by caspase-3, which resulted in significantly

lower fluorescence intensity found for cells treated with ST and inhibitor. These results confirm that the DMF NucView assay is specific for caspase 3.

## Conclusion

We present the first multiplexed cell-based screening assay implemented by digital microfluidics. Droplets of media containing HeLa cells were dispensed from reservoirs, moved, and seeded on adhesion pads by applying electric fields to an array of electrodes. Cell attachment and spreading characteristics on device surfaces were similar to those observed for standard polystyrene tissue culture surfaces. The passive dispensing technique was used to deliver model drugs and fluorescent reporters to cells cultured on DMF devices. The digital microfluidic passive dispensing technique was found to be superior to pipetting and aspiration for retaining weakly adhered apoptotic cells for analysis. A 6-plex caspase-3 activity assay was developed and implemented by digital microfluidics. The DMF platform outperformed an identical assay implemented in 96-well plate format, providing a larger dynamic range and  $\sim 33$  fold lower reagent consumption. These results suggest great potential for the application of digital microfluidics to cell-based screening in drug discovery. We anticipate that further development towards automation control of droplets actuation will make DMF technology an attractive solution for high-throughput screening in pharmaceutical research.

## Acknowledgements

We thank the Canadian Institute for Health Research (CIHR) and the Ontario Institute for Cancer Research for financial support. We thank Irwin A. Eydelnant for advice regarding liftoff patterning of Teflon-AF on ITO substrates. MDC thanks CIHR for a postdoctoral fellowship. IBN thanks the Natural Sciences and Engineering Research Council (NSERC) for a postdoctoral fellowship. ARW thanks the Canada Research Chair (CRC) program for a CRC.

## References

- 1 J. Drews, *Science*, 2000, **287**, 1960–1964.
- 2 R. Macarron, M. N. Banks, D. Bojanic, D. J. Burns, D. A. Cirovic, T. Garyantes, D. V. S. Green, R. P. Hertzberg, W. P. Janzen, J. W. Paslay, U. Schopfer and G. S. Sittampalam, *Nat. Rev. Drug Discovery*, 2011, **10**, 188–195.
- 3 K. A. Giuliano, R. L. DeBiasio, R. T. Dunlay, A. Gough, J. M. Volosky, J. Zock, G. N. Pavlakis and D. L. Taylor, *J. Biomol. Screening*, 1997, **2**, 249–259.
- 4 S. Laleh, *Frost & Sullivan*, 2008.
- 5 M. L. Yarmush and K. R. King, *Annu. Rev. Biomed. Eng.*, 2009, **11**, 235–257.
- 6 I. K. Dimov, G. Kijanka, Y. Park, J. Ducree, T. Kang and L. P. Lee, *Lab Chip*, 2011, **11**, 2701–2710.
- 7 M. W. Li and R. S. Martin, *Analyst*, 2008, **133**, 1358–1366.
- 8 S. L. Faley, M. Copland, J. Reboud and J. M. Cooper, *Biomechanics*, 2011, **5**, 024106–024107.
- 9 S. P. Forry, D. R. Reyes, M. Gaitan and L. E. Locascio, *J. Am. Chem. Soc.*, 2006, **128**, 13678–13679.
- 10 J. F. Lo, E. Sinkala and D. T. Eddington, *Lab Chip*, 2010, **10**, 2394–2401.
- 11 D. Wlodkowic, J. Skommer, D. McGuinness, S. Faley, W. Kolch, Z. Darzynkiewicz and J. M. Cooper, *Anal. Chem.*, 2009, **81**, 6952–6959.

- 12 D. Wlodkowic, K. Khoshmanesh, J. C. Sharpe, Z. Darzynkiewicz and J. M. Cooper, *Anal. Chem.*, 2011, **83**, 6439–6446.
- 13 N. Ye, J. Qin, W. Shi, X. Liu and B. Lin, *Lab Chip*, 2007, **7**, 1696–1704.
- 14 K. Khoshmanesh, J. Akagi, S. Nahavandi, J. Skommer, S. Baratchi, J. M. Cooper, K. Kalantar-Zadeh, D. E. Williams and D. Wlodkowic, *Anal. Chem.*, 2011, **83**, 2133–2144.
- 15 P. S. Ditttrich and A. Manz, *Nat. Rev. Drug Discovery*, 2006, **5**, 210–218.
- 16 S. I. Montanez-Sauri, K. E. Sung, J. P. Puccinelli, C. Pehlke and D. J. Beebe, *Journal of Laboratory Automation*, 2011, **16**, 171–185.
- 17 R. Fair, *Microfluid. Nanofluid.*, 2007, **3**, 245–281.
- 18 M. Abdelgawad and A. R. Wheeler, *Adv. Mater.*, 2009, **21**, 920–925.
- 19 A. R. Wheeler, *Science*, 2008, **322**, 539–540.
- 20 L. Malic, D. Brassard, T. Veres and M. Tabrizian, *Lab Chip*, 2010, **10**, 418–431.
- 21 A. R. Wheeler, H. Moon, C.-J. C. Kim, J. A. Loo and R. L. Garrell, *Anal. Chem.*, 2004, **76**, 4833–4838.
- 22 M. J. Jebraill and A. R. Wheeler, *Anal. Chem.*, 2008, **81**, 330–335.
- 23 V. N. Luk and A. R. Wheeler, *Anal. Chem.*, 2009, **81**, 4524–4530.
- 24 D. Chatterjee, A. J. Ytterberg, S. U. Son, J. A. Loo and R. L. Garrell, *Anal. Chem.*, 2010, **82**, 2095–2101.
- 25 V. Srinivasan, V. K. Pamula and R. B. Fair, *Lab Chip*, 2004, **4**, 310–315.
- 26 V. Srinivasan, V. K. Pamula and R. B. Fair, *Anal. Chim. Acta*, 2004, **507**, 145–150.
- 27 E. M. Miller and A. R. Wheeler, *Anal. Chem.*, 2008, **80**, 1614–1619.
- 28 Y.-H. Chang, G.-B. Lee, F.-C. Huang, Y.-Y. Chen and J.-L. Lin, *Biomed. Microdevices*, 2006, **8**, 215–225.
- 29 R. Sista, Z. Hua, P. Thwar, A. Sudarsan, V. Srinivasan, A. Eckhardt, M. Pollack and V. Pamula, *Lab Chip*, 2008, **8**, 2091–2104.
- 30 V. Schaller, A. Sanz-Velasco, A. Kalabukhov, J. F. Schneiderman, F. Oisjoen, A. Jesorka, A. P. Astalan, A. Krozer, C. Rusu, P. Enoksson and D. Winkler, *Lab Chip*, 2009, **9**, 3433–3436.
- 31 R. S. Sista, A. E. Eckhardt, V. Srinivasan, M. G. Pollack, S. Palanki and V. K. Pamula, *Lab Chip*, 2008, **8**, 2188–2196.
- 32 E. Miller, A. Ng, U. Uddayasankar and A. Wheeler, *Anal. Bioanal. Chem.*, 2011, **399**, 337–345.
- 33 N. A. Mousa, M. J. Jebraill, H. Yang, M. Abdelgawad, P. Metalnikov, J. Chen, A. R. Wheeler and R. F. Casper, *Sci. Transl. Med.*, 2009, **1**, 1ra2.
- 34 I. Barbulovic-Nad, H. Yang, P. S. Park and A. R. Wheeler, *Lab Chip*, 2008, **8**, 519–526.
- 35 S. U. Son and R. L. Garrell, *Lab Chip*, 2009, **9**, 2398–2401.
- 36 G. J. Shah, A. T. Ohta, E. P. Chiou, M. C. Wu and C. J. Kim, *Lab Chip*, 2009, **9**, 1732–1739.
- 37 I. Barbulovic-Nad, S. H. Au and A. R. Wheeler, *Lab Chip*, 2010, **10**, 1536–1542.
- 38 S. Au, S. Shih and A. Wheeler, *Biomed. Microdevices*, 2011, **13**, 41–50.
- 39 J. K. Valley, S. NingPei, A. Jamshidi, H.-Y. Hsu and M. C. Wu, *Lab Chip*, 2011, **11**, 1292–1297.
- 40 D. Witters, N. Vergauwe, S. Vermeir, F. Ceysens, S. Liekens, R. Puers and J. Lammertyn, *Lab Chip*, 2011, **11**, 2790–2794.
- 41 S. Srigunapalan, I. Eydelnant, C. Simmons and A. R. Wheeler, *Lab Chip*, 2012, DOI: 10.1039/C1LC20844F.
- 42 D. Hanahan and R. A. Weinberg, *Cell*, 2000, **100**, 57–70.
- 43 D. Hanahan and Robert A. Weinberg, *Cell*, 2011, **144**, 646–674.
- 44 *Apoptosis in Oncology: Drug Pipeline Update 2010*, BioSeeker Group AB, 2010.
- 45 K. M. Boatright and G. S. Salvesen, *Curr. Opin. Cell Biol.*, 2003, **15**, 725–731.
- 46 V. N. Luk, G. C. H. Mo and A. R. Wheeler, *Langmuir*, 2008, **24**, 6382–6389.
- 47 I. Eydelnant, U. Uddayasankar, B. Li, M. W. Liao and A. R. Wheeler, *Lab Chip*, 2012, DOI: 10.1039/C2LC21004E, in press.
- 48 C. Sung Kwon, M. Hyejin and K. Chang-Jin, *J. Microelectromech. Syst.*, 2003, **12**, 70–80.
- 49 G. W. Gross, W. Y. Wen and J. W. Lin, *J. Neurosci. Methods*, 1985, **15**, 243–252.
- 50 E. Bieberich and A. Guiseppi-Elie, *Biosens. Bioelectron.*, 2004, **19**, 923–931.
- 51 H. Pluk, D. J. Stokes, B. Lich, B. Wieringa and J. Fransen, *J. Microsc.*, 2009, **233**, 353–363.
- 52 S. S. Shah, M. C. Howland, L.-J. Chen, J. Silangcruz, S. V. Verkhoturov, E. A. Schweikert, A. N. Parikh and A. Revzin, *ACS Appl. Mater. Interfaces*, 2009, **1**, 2592–2601.
- 53 H.-W. Lu, F. Bottausci, J. D. Fowler, A. L. Bertozzi, M. Carl and C.-J. C. Kim, *Lab Chip*, 2008, **8**, 456–461.
- 54 N. A. Thornberry and Y. Lazebnik, *Science*, 1998, **281**, 1312–1316.
- 55 S. Kumar, *Clin. Exp. Pharmacol. Physiol.*, 1999, **26**, 295–303.
- 56 H. Cen, F. Mao, I. Aronchik, R. J. Fuentes and G. L. Firestone, *FASEB J.*, 2008, **22**, 2243–2252.